JOURNAL OF CATALYSIS 34, 246–256 (1974)

Isobaric Diffusion, Permeability, and Simultaneous Flow and Diffusion in Commercial Catalysts

RAN ABED* AND ROBERT G. RINKER

Department of Chemical and Nuclear Engineering, University of California, Santa Barbara, California 93106

Received December 14, 1973

An experimental study of isobaric binary diffusion, permeability of pure gases, and simultaneous flow and binary diffusion in commercial catalyst pellets was conducted at pressures up to 48 atm. Attempts to correlate the data, using the dusty-gas model and its extended form, showed that an additional constant, τ, must be introduced into the model. This constant is directly measurable and is a function of only the pellet structure. Furthermore, all the constants in the model can be determined from isobaric diffusion and permeability measurements and then used directly to describe the fluxes for simultaneous diffusion and flow.

NOMENCLATURE

a, a'	Grouping terms defined by Eqs. (15) and (17), respectively, g-mole/cm-sec
A	Component A
b, b'	Grouping of terms defined by Eqs. (16) and (18), respectively, g-mole-cm/dyn-sec
B	Component B
C_0	Constant dependent only upon structure of porous medium and giving relative D'Arcy flow permeability, cm^2
C_1	Constant dependent only upon structure of porous medium and giving relative Knudsen flow permeability, cm
C_2	Constant dependent only upon structure of porous medium and giving ratio of molecular diffusivity within the porous medium to the free gas diffusivity, dimensionless
C_3	Ratio defined by Eq. (26), cm
C_4	Ratio defined by Eq. (27), cm^2
D_{AB}	Free gas mutual diffusivity in a binary mixture of components A and B, cm^2/sec
D_{AB}^0	Pressure independent mutual diffusivity defined by Equation (1d), dyn/sec
G	Grouping of terms defined by Eq. (6), dimensionless.
K_A	Effective Knudsen diffusivity defined by Eq. (1a), cm^2/sec
K_B	Effective Knudsen diffusivity defined by Eq. (1b), cm^2/sec
K'_A	Grouping of terms defined by Eq. (23), cm/sec
K'_B	Grouping of terms defined by Eq. (24), cm/sec
K_m	Mixture effective Knudsen diffusivity defined by Eq. (1c), cm^2/sec
K'_m	Grouping of terms defined by Eq. (25), cm/sec
L	Length of the catalyst pellet, cm
M	Molecular weight, g/g-mole
N	Molar flux, g-moles/cm^2-sec
P	Total pressure, dyn/cm^2
P_0	Total pressure at the same position as taken for y_{A_0}, dyn/cm^2
P_L	Total pressure at the same position as taken for y_{A_L}, dyn/cm^2
R_g	Gas constant, 8.31×10^7 ergs/g-mole-°K
S	Grouping of terms defined by Eq. (8), dimensionless
T	Absolute temperature, °K
y	Mole fraction

* Present address: E. I. duPont de Nemours & Co., Engineering Technology Laboratory, Wilmington, DE 19898.

y_{A_L} Mole fraction of component A at $Z = L$ of the pellet
y_{A_0} Mole fraction of component A at $Z = 0$
Z Distance in direction of mass transfer, cm
μ Viscosity, g/cm-sec
τ Constant dependent only upon structure of porous medium and corrects slip-flow term in dusty-gas model, dimensionless

Subscripts

A Component A
B Component B
L Value at $Z = L$
m Mixture
0 Value at $Z = 0$ (does not apply to C_0)

Introduction

There are mainly three models in use for describing diffusion and flow of gases in porous solids. They include the parallel-path pore model, the random pore model, and the dusty-gas model. A comprehensive review of these models is provided by Youngquist (*1*).

The random pore model was proposed by Wakao and Smith (*2*) and is predictive in nature. They applied it successfully, as did Henry, Cunningham and Geankoplis (*3*) and Cunningham and Geankoplis (*4*), to the prediction of isobaric fluxes in bidispersed pore systems which were prepared in the laboratory by compressing powder particles that are themselves porous. Otani, Wakao and Smith (*5*) extended the model to simultaneous flow and diffusion in porous media and again found good agreement between the model and data for bimodal systems.

According to Satterfield and Cadle (*6*) a comparison of the random pore model with the parallel-path pore model showed that the latter is superior in predicting isobaric diffusion fluxes in commercial catalyst pellets. This was confirmed later by Brown, Haynes and Manogue (*7*).

In further work, Satterfield and Cadle (*8*) performed simultaneous diffusion and flow experiments on commercial catalysts and correlated their data with the parallel-path pore model applied to an equation for diffusion and flow derived by Evans, Watson and Mason (*9*) in terms of a dusty-gas constant. They also applied the parallel-path pore model to a capillary-tube flow equation derived by Wakao, Otani and Smith (*10*). They observed that the diffusion tortuosity factor was about 1.8 times as large as the flow-term tortuosity.

The dusty-gas model was conceived by Deriaguin (*11*) for uniform, isotropic porous media. Evans, Watson and Mason (*12*) derived a simpler version but based on the same ideas. Extension of the dusty-gas model to simultaneous diffusion and flow in porous media has been reported by Mason, Malinauskas and Evans (*13*) and independently by Gunn and King (*14*).

More recently, Omata and Brown (*15*) applied the dusty-gas model to isobaric diffusion in unimodal as well as bimodal structures. In unimodal structures with pore sizes below 50 Å, they observed a deviation between computed and experimental fluxes. In bimodal structures, a deviation was also observed; and it was suggested that an additional cause may be attributed to the fact that the systems contained micro- and macropores in parallel.

In the work reported here, we chose to apply the extended form of the dusty-gas model to commercial, bimodal catalyst pellets.

To check the conclusions of Omata and Brown (*15*) we chose Girdler T-126 γ-alumina pellets because of their highly microporous structure and T-708 α-alumina pellets because of their highly macroporous structures. To extend their work, which included isobaric diffusion measurements at different pressures and temperatures, we chose to perform not only isobaric diffusion experiments but also permeability experiments as well as simultaneous diffusion and flow experiments. The main purpose in this approach was to investigate whether or not the constants obtained from the separate diffusion and permeability measurements can be used to describe simultaneous diffusion and flow fluxes in commercial catalyst pellets.

Experimental measurements of effective

diffusivities in porous solids are most commonly conducted at steady conditions in an apparatus similar to that developed by Wicke and Kallenbach (*16*) and later modified by Weisz (*17*). Transient measurements are also made by means of gas chromatography (*18–20*) or by the "time-lag" method (*21*).

In the present work, a modified version of the Wicke–Kallenbach cell was designed. An important modification of the design includes the use of agitators similar to those used by Gunn and King (*14*) in each compartment, with magnetic coupling to the external drive-motors. With essentially complete mixing in each compartment, as well as depletion of the boundary-layer resistance, it is possible to use moderate flow rates and hence maintain adequate concentrations of diffusing species. The higher concentrations, compared to those obtained at high flow rates, greatly improve the accuracy of detection by gas chromatography. The magnetic coupling permits high-pressure operation with minimal chances of leakage.

Another important modification is the inclusion of up to 10 pellets (0.25-in. diam) which can be sealed by a rubber partition similar to that used by Satterfield and Cadle (*6*).

Apparatus

The diffusion cell consists of two cylindrical compartments separated by a rubber partition and is designed to operate at pressures up to 1000 psig. It can easily be disassembled for adding or replacing up to 10 cylindrical pellets (0.25-in. diam) which are inserted into the rubber partition. Only the circular ends of the pellets are exposed to each compartment, since the partition thickness is selected to cover and seal the entire cylindrical sides. To verify the absence of leakage around the pellets, tests were made with pellets having epoxy-sealed ends, with liquid-filled pellets and finally with brass pellets (*22*).

Each compartment, having a volume of approximately 500 cc, contains an impeller assembly with a magnet mounted on the drive shaft. These magnets provide the coupling to the outside motors also fitted with magnets attached to their drive shafts. Rotating speeds up to 1750 rpm are available. The coupling occurs through the 1-in. thick end-plates; and a helmholz coil imbedded in each end-plate provides an electrical signal to a sensitive rms voltmeter when the magnetic fields are coupled. The entire cell assembly is held together with eight (0.75-in. diam) tie-bolts through the oversized end-plates. Seals between each major part are provided by O-rings.

A flow diagram of the system is shown in Fig. 1. Considering the flow through one compartment, pure gas from a high-pressure cylinder (A) is supplied to an APCO Model 1B precision, high-pressure regulator (B) where the pressure is reduced to the cell-operating value. The gas leaving the cell compartment (C) passes first through a Matheson Model 8-590 two-stage regulator (D) followed by a micrometer, needle-valve (E) for flow regulation. It then moves to a sampling subsystem (F) which is connected to a Loenco Model 160 gas chromatograph (G). The gas leaving the sampling system travels finally through a soap-bubble meter or to a wet-test meter

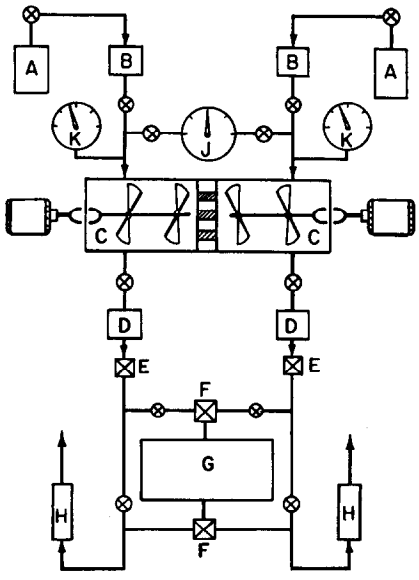

Fig. 1. Flow diagram of diffusion apparatus.

(H) for flow-rate measurement and is discharged to the ambient pressure. Flow through the second compartment follows a parallel scheme.

Measurement of small pressure differences between the compartments is accomplished with a Barton Model 200 differential pressure gage (J) which has a range of -10 to $+20$ in. of water column and is capable of detecting pressure differences of as low as 0.1 in. of water column. Larger pressure drops are measured by a Barton Model 200 differential pressure gage with a range of 0 to 5 psi readable to ± 0.02 psi. The total operating pressure on the cell is measured with a Heise gauge (K) with a range of 0 to 1000 psig and readable to ± 1 psig.

Measurement of temperature to better than ± 0.05°C is accomplished with thermocouples inserted into the cell and monitored with a Leeds and Northrup Model K-3 potentiometer facility. Thermocouples are also inserted into the exit stream of each bubble-flow meter. All experiments reported here were conducted at or near 25°C.

The two diffusing gases used in this study are nitrogen and helium with purities of 99.995% and obtained from Matheson, Inc. Argon of the same purity has been used in the permeability experiments. Analyses of nitrogen–helium mixtures from the diffusion cell are accomplished in the gas chromatograph by first separating them on a column which is 12 ft long by 0.25-in. in diameter and is packed with a 50–50 mixture of molecular sieves 4A and 5A, 60–80 mesh. Hydrogen is the carrier gas, and the column temperature is 60°C. The separated species are detected with a sensitive katharometer. Retention times and areas under the chromatograms are recorded by a Hewlett-Packard Model 3370A digital integrator.

All measuring equipment has been carefully calibrated by standard methods. The error for any *single* measurement involved in any given diffusion or permeability or simultaneous diffusion–permeability experiment is maintained between limits of $\pm 2\%$. Errors in flux measurements which include concentrations and flow rates may be as high as $\pm 3\%$.

Experimental Procedure

In a typical run, the cell is loaded with 8 pellets, reassembled and carefully tested for leaks with helium. It is then evacuated and finally brought up to operating pressure by simultaneously feeding each compartment with the diffusing components. In permeability experiments, only a single component is used. After setting the speed of agitation and assuring that the magnetic fields are coupled, the gas flows are adjusted to predetermined rates.

Steady state is usually reached in approximately 3 hr depending on the flow rate of gases and on the operating pressure in the cell compartments. Periodic checks of the gas composition in each compartment are used to determine when steady state is achieved.

Typically, the measurements required for calculating C_0, C_1 and C_2 and subsequently the effective diffusivities, in a simultaneous diffusion–permeability experiment, include the composition and flow rates of mixtures leaving each compartment, the total cell pressure and temperature, and the pressure drop across the pellets. To obtain the gas composition, each stream is periodically diverted to the calibrated sample loop of the gas chromatograph wherein a known quantity is collected for analysis.

Viscosities of the pure components are obtained from published data (*23*).

Theory

The proposed equation for describing the flux of component A as a result of steady diffusion and flow in a general porous medium is as follows:

$$\mathbf{N}_A = -\frac{C_2 D_{AB}^0 K_A P}{(C_2 D_{AB}^0 + K_m P) R_g T} \nabla y_A - \left[\frac{\tau K_A (C_2 D_{AB}^0 + K_B P)}{C_2 D_{AB}^0 + K_m P} + \frac{C_0 P}{\mu_m} \right] \frac{y_A}{R_g T} \nabla P, \quad (1)$$

where

$$K_A = C_1 (R_g T / M_A)^{1/2}, \quad (1a)$$

$$K_B = C_1 (R_g T / M_B)^{1/2}, \quad (1b)$$

$$K_m = y_B K_A + y_A K_B, \quad (1c)$$

$$D_{AB}^0 = D_{AB} P. \quad (1d)$$

The constant, C_1, has units of length and can be thought of as an "effective" Knudsen radius. A knowledge of its value allows one to calculate the effective Knudsen diffusivity from Eq. (1a) or (1b). The dusty-gas constant, C_2, is dimensionless and is essentially the ratio of the effective molecular diffusivity to the free-space molecular diffusivity. A knowledge of its value allows one to calculate the effective molecular diffusivity in the system. The D'Arcy constant, C_0, has units of length-squared and is a measure of the effective permeability.

The difference between Eq. (1) and the one proposed by Gunn and King (*14*) is the inclusion of an additional constant, τ. Our basis for introducing τ is, at present, mainly experimental. A detailed series of experiments have shown that τ is required when the extended form of the dusty-gas model is applied to bimodal commercial pellets. As confirmed by Gunn and King (*14*) the value of τ is unity for unimodal macroporous structures to which the dusty-gas model rigorously applies.

To test Eq. (1), we have applied it to data for one-dimensional systems under isothermal, steady-state conditions. The experiments have included isobaric diffusion of a two-component system, permeability of a single component, and finally simultaneous diffusion and permeability of a two-component system. For isobaric diffusion, $\nabla P = 0$; and Eq. (1) reduces to the following expression:

$$\mathbf{N}_A = -\frac{C_2 D_{AB}^0 K_A P}{(C_2 D_{AB}^0 + K_m P) R_g T}\left(\frac{dy_A}{dZ}\right). \quad (2)$$

The boundary conditions for Eq. (2) are:

$$\text{at } Z = 0, \quad y_A = y_{A_0} \quad (3)$$

$$\text{at } Z = L, \quad y_A = y_{A_L}. \quad (4)$$

Substitution of Eqs. (3) and (4) into the integrated form of Eq. (2) gives,

$$\mathbf{N}_A = \frac{P C_2 D_{AB}}{R_g T L G} \ln\left(\frac{1 - G y_{A_L} + C_2 D_{AB}/K_A}{1 - G y_{A_0} + C_2 D_{AB}/K_A}\right), \quad (5)$$

where G is given by,

$$G = 1 + \mathbf{N}_B/\mathbf{N}_A = 1 - (M_A/M_B)^{1/2}. \quad (6)$$

The relationship between the flux ratio and the molecular weight ratio shown in the definition of G in Eq. (6) applies to a counter-diffusing binary system and is true whether the transport mechanism is by pure Knudsen flow or by pure molecular diffusion or in the transition region. The relationship is useful in checking consistency of experimental data when both fluxes are measured independently. Deviations from the theoretical ratio may be attributed to measurement errors or to surface diffusion.

Equation (5) can be rearranged and written as follows:

$$\left[\frac{(y_{A_0} e^S - y_{A_L})G}{(e^S - 1) D_{AB}^0} - \frac{1}{D_{AB}^0}\right]\left(\frac{R_g T}{M_A}\right)^{1/2} = \frac{C_2}{C_1 P}, \quad (7)$$

where

$$S = \mathbf{N}_A R_g T L G / C_2 D_{AB}^0. \quad (8)$$

A plot of the left side of Eq. (7) versus $1/P$ yields a straight line that passes through the origin, with a slope of C_2/C_1. We have adopted this linearization procedure only for the purpose of finding approximate values of C_1 and C_2. Our estimate of C_2 was made by noting in Eq. (5) that the term, $C_2 D_{AB}/K_A$, is small relative to other terms in the logarithmic factor at high pressures, thus allowing direct calculation of C_2. We then applied a nonlinear regression technique (*24*) on Eq. (5) over the entire pressure range for the final evaluation of C_1 and C_2.

For permeability of pure gases, Eq. (1) for the flux of pure component A reduces to

$$\mathbf{N}_A = -\left(\tau K_A + \frac{C_0 P}{\mu_A}\right)\frac{1}{R_g T}\frac{dP}{dZ}. \quad (9)$$

The boundary conditions for Eq. (9) are:

$$P = P_0 \text{ at } Z = 0, \quad (10)$$

$$P = P_L \text{ at } Z = L. \quad (11)$$

Integration of Eq. (9) and substitution of the boundary conditions (10) and (11) gives,

$$\frac{\mathbf{N}_A(M_A R_g T)^{1/2}}{P_0 - P_L} = \frac{\tau C_1}{L} + \frac{C_0}{L^2}\left[\frac{(P_0 + P_L)L}{2\mu_A}\left(\frac{M_A}{R_g T}\right)^{1/2}\right]. \quad (12)$$

A plot of

$$\frac{\mathbf{N}_A(M_A R_g T)^{1/2}}{P_0 - P_L}$$

versus

$$\frac{P_0 + P_L}{2\mu_A}\left(\frac{M_A}{R_g T}\right)^{1/2} L$$

yields a straight line with an intercept of $\tau C_1/L$ and a slope of C_0/L^2. Knowing the value of C_1 from isobaric diffusion experiments enables the evaluation of τ.

Finally, for simultaneous steady diffusion and flow, we can write the flux Eq. (1) for components A and B in compressed form as follows:

$$\mathbf{N}_A = -a\frac{dy_A}{dZ} - b\frac{dP}{dZ}, \quad (13)$$

$$\mathbf{N}_B = -a'\frac{dy_B}{dZ} - b'\frac{dP}{dZ}, \quad (14)$$

where a, a', b, and b' are defined as follows:

$$a = \frac{C_2 D_{AB}{}^0 K_A P}{(C_2 D_{AB}{}^0 + K_m P)R_g T}, \quad (15)$$

$$b = \left[\frac{\tau K_A(C_2 D_{AB}{}^0 + K_B P)}{C_2 D_{AB}{}^0 + K_m P} + \frac{C_0 P}{\mu_m}\right]\frac{y_A}{R_g T}, \quad (16)$$

$$a' = \frac{C_2 D_{AB}{}^0 K_B P}{(C_2 D_{AB}{}^0 + K_m P)R_g T}, \quad (17)$$

$$b' = \left[\frac{\tau K_B(C_2 D_{AB}{}^0 + K_A P)}{C_2 D_{AB}{}^0 + K_m P} + \frac{C_0 P}{\mu_m}\right]\frac{y_B}{R_g T}. \quad (18)$$

Noting that for a binary system, $y_A + y_B = 1$ and also that $dy_A/dZ = -dy_B/dZ$, we can substitute these relationships into Eq. (14) to obtain,

$$\mathbf{N}_B = a'\frac{dy_A}{dZ} - b'\frac{dP}{dZ}. \quad (19)$$

Equations (13) and (19) can then be solved for dP/dZ and dy_A/dZ to give,

$$\frac{dP}{dZ} = -\frac{a\mathbf{N}_B + a'\mathbf{N}_A}{ab' + a'b}, \quad (20)$$

$$\frac{dy_A}{dZ} = \frac{b\mathbf{N}_B - b'\mathbf{N}_A}{ab' + a'b}. \quad (21)$$

In order to establish a direct relationship between the variables P and y_A, we can divide Eq. (20) by Eq. (21) and solve for dP/dy_A:

$$\frac{dP}{dy_A} = -\frac{a\mathbf{N}_B + a'\mathbf{N}_A}{b\mathbf{N}_B - b'\mathbf{N}_A}. \quad (22)$$

By defining the following quantities,

$$K'_A = (R_g T/M_A)^{1/2}, \quad (23)$$

$$K'_B = (R_g T/M_B)^{1/2}, \quad (24)$$

$$K'_m = y_A K'_B + y_B K'_A, \quad (25)$$

$$C_3 = C_1/C_2, \quad (26)$$

$$C_4 = C_0/C_1, \quad (27)$$

and by substituting Eqs. (15), (16), (17), (18), (23), (24), (25), (26), and (27) into Eq. (22) we obtain a working expression which can be integrated numerically,

$$\frac{dP}{dy_A} = D_{AB}{}^0 P(K'_A\mathbf{N}_B + K'_B\mathbf{N}_A) \Big/ \Big\{\tau D_{AB}{}^0 \times [K'_B(1 - y_A)\mathbf{N}_A - K'_A y_A \mathbf{N}_B] + [(1 - y_A)\mathbf{N}_A - y_A\mathbf{N}_B]\Big(C_3\tau K'_A K'_B P + C_4\frac{P}{\mu_m}D_{AB}{}^0 + C_3 C_4\frac{P^2}{\mu_m}K'_m\Big)\Big\}. \quad (28)$$

It is important to note that Eq. (28) has only three constants, namely, τ, C_3 and C_4. The integration of Eq. (28) has been performed numerically using the following stepwise procedure:

1. A value for τ obtained from permeability and isobaric diffusion experiments is substituted into Eq. (28).

2. Integration of Eq. (28) is performed from $y_A = y_{A_0}$ and $P = P_0$ to $y_A = y_{A_L}$; and the result of the integration gives a computed value of the pressure P_L, at $y_A = y_{A_L}$.

3. A nonlinear regression technique (*24*) is applied for the evaluation of the constants C_3 and C_4 using $(P_0 - P_L)$ as the dependent variable. In this procedure, the computer program finds the values of C_3

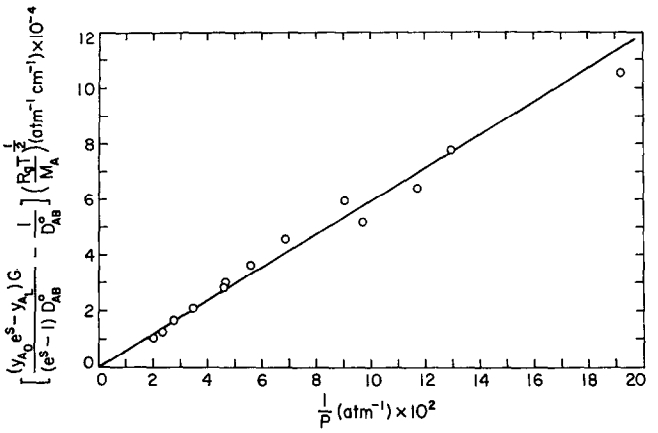

FIG. 2. Diffusion relationship in Girdler pellet Type T-126 (A = helium; B = nitrogen).

and C_4 which minimize the sum of the squares of the differences between computed and observed $(P_0 - P_L)$.

4. The viscosity of a mixture μ_m can be computed by the following correlation (*25*):

$$\mu_m = \frac{(\mu_A y_A M_A^{1/2} + \mu_B y_B M_B^{1/2})}{(y_A M_A^{1/2} + y_B M_B^{1/2})}. \quad (29)$$

RESULTS

The porous media which were investigated in this work are 0.25 × 0.25 in. commercial catalytic pellets manufactured by Girdler Catalysts Division of Chemetron Corp. The physical properties of the T-126 pellets are described by Satterfield and Cadle (*6*) as well as by Haynes (*26*) and those of the T-708 pellets are described by Abed (*27*). It is important to note that the T-126 pellet is highly microporous since 61% of its pore volume is in pores with diameters below 50 Å (*26*). The T-708 pellet is moderately macroporous and has 65% of its pore volume in pores with diameters between 800 and 1800 Å (*27*). Consequently, the T-126 pellet has a much larger surface area per gram than the T-708 pellet.

We will first consider the results of the isobaric diffusion experiments, which were all conducted at room temperature. The diffusing gases were helium and nitrogen. For the T-126 pellets, the flux ratio (helium/nitrogen) varied between 2.54 to 2.70 which is within ±4% of the theoretical value of 2.65. For the T-708 pellets, the flux ratio varied from 2.56 to 2.78 which is still within our overall experimental error. The variation of the flux ratios with pressure for both pellets showed no trend; and from this, we concluded that surface diffusion made no significant contributions to the fluxes.

Figure 2 includes all the data points for the T-126 pellets. In this figure, the left side of Eq. (7) is plotted versus $1/P$, and the slope of the line is C_2/C_1. The values of C_1 and C_2 used in preparing Fig. 2 were computed by applying the nonlinear regression technique to Eq. (5), wherein the helium flux, $\mathbf{N}_{He}$, was taken as the dependent variable. In another computation, the nitrogen flux $\mathbf{N}_{N_2}$, was taken as the dependent variable. The difference between the values of C_1 and C_2 based on each of

TABLE 1
RESULTS FROM ISOBARIC DIFFUSION OF HELIUM AND NITROGEN AT ROOM TEMPERATURE

Girdler pellet type	Pressure range (atm)	$C_1 \times 10^8$ (cm)	C_2	$(C_1/C_2) \times 10^8$ (cm)
T-126 0.25 × 0.25 in.	5–48	26.4 ± 2.6	0.166 ± 0.008	159 ± 24
T-708 0.25 × 0.25 in.	6–42	202 ± 20	0.342 ± 0.017	590 ± 88

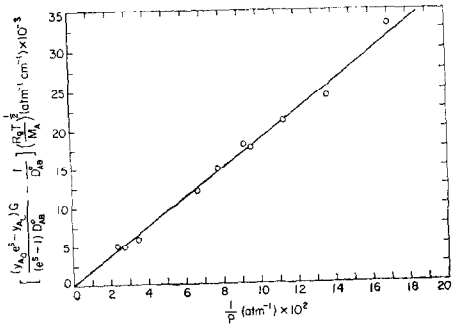

FIG. 3. Diffusion relationship in Girdler pellet Type T-708 (A = helium; B = nitrogen).

the fluxes is well within our experimental error. Hence, the arithmetic averages of both values of C_1 and C_2 and their respective error bounds are listed in Table 1.

Figure 3 includes the data points for the T-708 pellets and was prepared by using the C_1 and C_2 values based on the helium fluxes.

The results of the nonlinear regression analysis show that there is a good correlation between the dusty-gas model and the data. The maximum relative deviation between the computed and the observed fluxes of helium was 0.05 for the T-126 pellet and 0.018 for the T-708 pellet. This deviation is defined as:

$$\text{rel. dev.} = \frac{\text{obsd flux} - \text{calcd flux}}{\text{calcd flux}}. \quad (30)$$

The fact that the deviation for the T-126 pellet is larger than for the T-708 would be expected based on the conclusions of Omata and Brown (*15*). Also our computed tortuosity factor of 3.2 for the T-126 pellet is in reasonable agreement with a value of 3.6 obtained by Satterfield and Cadle (*6*).

Regarding the error estimate of C_1 and C_2, the relative error in C_1 is larger than that for C_2. This is attributed to the fact that the computed fluxes in our pressure range are more sensitive to C_2 than to C_1. More accurate values of C_1 could have been obtained by taking data points at very low pressures as was done in the work of Gunn and King (*14*).

We will next consider the results from the permeability experiments, which again were conducted at room temperature. In order to check the independence of the constants, τ, C_1 and C_0, on the flowing material, the flow of three different gases, nitrogen, helium and argon, was measured. Figure 4 includes data points for the T-126 pellets. In this case, results from the flow of helium and argon (nitrogen was not used) fall on one line. The intercept of the straight line is $\tau C_1/L$, and the slope is C_0/L^2. Knowing the value of C_1 from the isobaric diffusion experiments permits the computation of τ.

Figure 5 shows the results from the permeability of helium, argon and nitrogen in the T-708 pellets. Both Figs. 4 and 5

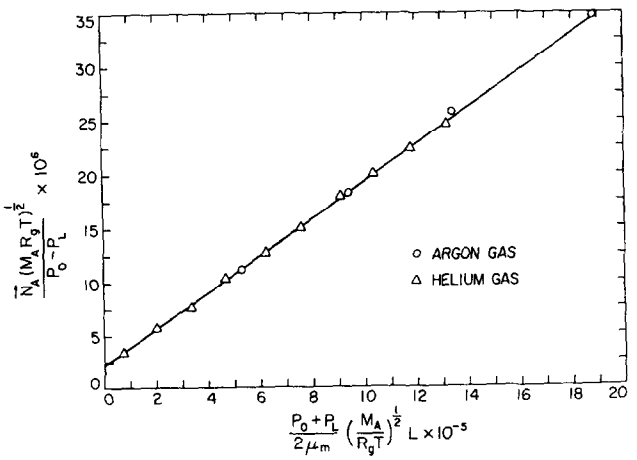

FIG. 4. Permeability of Girdler pellet Type T-126.

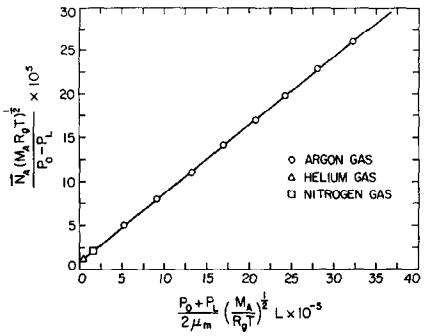

FIG. 5. Permeability of Girdler pellet Type T-708.

are based on a linear least-square analysis of the data, and the data points correlate extremely well with the model.

The results of the permeability experiments in the T-126 and T-708 pellets are summarized in Table 2. Note that the value of τ for the T-126 pellets is larger than for the T-708 pellets by a factor of 2.1. This could be attributed to the fact that the T-126 pellet is much more microporous and less homogeneous than the T-708 pellet.

In checking on the appropriateness of τ, a value of $C_1 = 129 \times 10^{-8}$ cm, calculated from the permeability data on the T-126 pellets, was used in a regression analysis of the isobaric diffusion data with C_2 as a single adjustable parameter. The resulting value, $C_2 = 0.116$, was 25% lower than the value reported in Table 1 and predicted a tortuosity factor of 4.5, which is considerably higher than the reported value (*6*). Moreover, the relative deviation of C_2 computed as a single parameter was found to correlate with pressure and had a maximum relative deviation of 31%. Since no experimental error could be correlated with pressure and since C_2 is a function only of pore structure, we conclude that C_1 evaluated from permeability data cannot be used to obtain C_2 from isobaric diffusion data for bimodal structures, especially those with significant contributions from micropores.

We will finally consider the results of experiments wherein both flow and diffusion are simultaneously taking place. The purpose of these experiments was to show that the constants obtained by the separate isobaric diffusion and permeability measurements can be used to describe the fluxes for simultaneous diffusion and flow. With this in mind, the final results of the simultaneous flow and diffusion experiments are summarized in Table 3. Since helium was on the high-pressure side, the flux ratio, $-\mathbf{N}_{He}/\mathbf{N}_{N_2}$, is much larger than the theoretical flux ratio in the isobaric diffusion case. This means that the contribution of bulk flow to the helium fluxes dominates. On the other hand, the nitrogen fluxes are due primarily to diffusion.

The results of the nonlinear regression analysis show very good agreement between the model and the data. The maximum relative deviation between the observed and computed pressure difference across the pellet is 0.06 for the T-126 pellets which is significantly higher than the value of 0.022 for the T-708 pellets. Again, this would be expected based on the conclusions of Omata and Brown (*15*).

The two constants which are evaluated as a result of these experiments are $C_3 = C_1/C_2$ and $C_4 = C_0/C_1$; and their values are listed in Table 3. Note that τ was held constant at its values obtained in the previous experiments. It is clear from these results that there is fair agreement between the values of C_3 and C_4 obtained by these experiments and those obtained from isobaric diffusion and from permeability ex-

TABLE 2

RESULTS FROM PERMEABILITY OF PURE GASES—ARGON, HELIUM AND NITROGEN—AT ROOM TEMPERATURE

Girdler pellet type	Pressure range (atm)	Pressure drop range (psia)	τ	$C_0 \times 10^{11}$ (cm²)	$(C_0/C_1) \times 10^5$ (cm)
T-126 0.25 × 0.25 in.	2–32	1.6–4.4	4.9 ± 0.7	0.698 ± 0.035	2.65 ± 0.40
T-708 0.25 × 0.25 in.	1–29	6–10	2.3 ± 0.3	3.17 ± 0.16	1.57 ± 0.23

TABLE 3
RESULTS FROM SIMULTANEOUS FLOW AND DIFFUSION OF HELIUM AND NITROGEN EXPERIMENTS AT ROOM TEMPERATURE

Girdler pellet type	Pressure range (atm)	Flux ratio $-N_{He}/N_{N_2}$	Pressure drop range (psia)	$C_3 \times 10^8$ (cm)	$C_4 \times 10^5$ (cm)
T-126 0.25 × 0.25 in.	5–28	13–46	1.7–2.6	212 ± 32	2.63 ± 0.40
T-708 0.25 × 0.25 in.	6–25	17–33	1.5–3.5	580 ± 87	1.35 ± 0.20

periments for the highly microporous T-126 pellets whereas the agreement is good for the T-708 pellets.

It is important to note that there are two sources of error in the evaluation of C_3 and C_4 from the simultaneous diffusion and flow experiments. One is the experimental error; and the other is the error in τ, which was assumed to be constant in the regression analysis.

A sensitivity analysis of C_3 and C_4 evaluated from the simultaneous diffusion and flow data shows them to be sensitive to τ. For example, decreasing τ for the T-126 pellets by 15%, which is our reported lower bound, gives $C_3 = 187 \times 10^{-8}$ cm and $C_4 = 2.94 \times 10^{-5}$ cm. The former constant approaches the value obtained from the isobaric diffusion experiments and reported as C_1/C_2 in Table 1, whereas the latter constant diverges from the value obtained from the permeability experiments and reported as C_0/C_1 in Table 2. Further lowering of τ causes the divergence of C_4 to rapidly increase. Hence, the reported τ is within the correct range bounded by our experimental errors.

CONCLUSIONS

The extended dusty-gas model can be successfully applied to bimodal, commercial catalyst pellets. This requires an additional constant, τ, which represents the ratio of the effective Knudsen radius evaluated from permeability of pure gases to the effective Knudsen radius evaluated from isobaric diffusion of binary mixtures. Furthermore, the four constants, C_0, C_1, C_2 and τ, can be determined from isobaric diffusion and permeability measurements and then used with fair accuracy to describe the fluxes for simultaneous diffusion and flow.

ACKNOWLEDGMENTS

The authors express their appreciation to the National Science Foundation for support of this work under NSF Grant GK 25570. Catalysts were supplied by J. H. Miller, Girdler Catalysts Division of Chemetron Corp. The authors also express their appreciation to Professor Henry W. Haynes Jr., for helpful suggestions and discussions.

REFERENCES

1. YOUNGQUIST, G. R., *Ind. Eng. Chem.* **62**, 52 (1970).
2. WAKAO, N., AND SMITH, J. M., *Chem. Eng. Sci.* **17**, 825 (1962).
3. HENRY, J. P., CUNNINGHAM, R. S., AND GEANKOPLIS, C. J., *Chem. Eng. Sci.* **22**, 11 (1967).
4. CUNNINGHAM, R. S., AND GEANKOPLIS, C. J., *Ind. Eng. Chem., Fundam.* **7**, 535 (1968).
5. OTANI, S., WAKAO, N., AND SMITH, J. M., *AIChE J.* **11**, 439 (1965).
6. SATTERFIELD, C. N., AND CADLE, P. J., *Ind. Eng. Chem., Process Des. Develop.* **7**, 256 (1968).
7. BROWN, L. F., HAYNES, H. W., AND MANOGUE, W. H., *J. Catal.* **14**, 220 (1969).
8. SATTERFIELD, C. N., AND CADLE, P. J., *Ind. Eng. Chem., Fundam.* **7**, 202 (1968).
9. EVANS, R. B., III, WATSON, G. M., AND MASON, E. A., *J. Chem. Phys.* **36**, 1894 (1962).
10. WAKAO, N., OTANI, S., AND SMITH, J. M., *AIChE J.* **11**, 435 (1965).
11. DERIAGUIN, B. V., *Dokl. Akad. Nauk USSR* **53**, 627 (1946).
12. EVANS, R. B., III, WATSON, G. M., AND MASON, E. A., *J. Chem. Phys.* **35**, 2076 (1961).
13. MASON, E. A., MALINAUSKAS, A. P., AND EVANS, R. B., III, *J. Chem. Phys.* **46**, 3199 (1967).
14. GUNN, R. D., AND KING, C. J., *AIChE J.* **15**, 507 (1969).
15. OMATA, H., AND BROWN, L. F., *AIChE J.* **18**, 967 (1972).

16. WICKE, E., AND KALLENBACH, R., *Kolloid Z.* **97,** 135 (1941).
17. WEISZ, P. B., *Z. Phys. Chem.* **11,** 1 (1957).
18. DAVIS, R. B., AND SCOTT, D. S., *in* "Symposium on Fundamentals of Heat and Mass Transfer," p. 21. 58th Annu. Meet., AIChE, Philadelphia, PA, 1965.
19. DAVIS, R. B., AND SCOTT, D. S., *in* "Symposium on Porous Structure and Catalytic Transport Processes in Heterogeneous Catalysis" (G. K. Boreskov, Ed.), Akad. Kiado, Budapest, 1972.
20. SCHNEIDER, P., AND SMITH, J. M., *AIChE J.* **14,** 762 (1968).
21. BARRER, R. M., *J. Phys. Chem.* **57,** 35 (1953).
22. ABED, R., AND RINKER, R. G., *J. Catal.* **31,** 119 (1973).
23. KESTIN, J., AND LEIDENFROST, W., *Physica* **25,** 1033 (1959).
24. BAER, R. M., "Nonlinear Regression," G2-CAL-NLIN, Computer Center, University of California, Berkeley, June, 1967.
25. HERNING, J., AND ZIPPERER, L., *Gas Wasserfach.* **79,** 49 (1936).
26. HAYNES, H. W., JR., PhD thesis, Univ. of Colorado, Boulder, CO, 1969.
27. ABED, R., PhD thesis, Univ. of California, Santa Barbara, CA, 1973.